Interferometer measurements of terahertz waves from $Bi_2Sr_2CaCu_2O_{8+d}$ mesas

2012 Supercond. Sci. Technol. 25 125004

(http://iopscience.iop.org/0953-2048/25/12/125004)

Supercond. Sci. Technol. **25** (2012) 125004 (5pp) doi:10.1088/0953-2048/25/12/125004

Interferometer measurements of terahertz waves from $Bi_2Sr_2CaCu_2O_{8+d}$ mesas

F Turkoglu[1], H Koseoglu[1], Y Demirhan[1], L Ozyuzer[1], S Preu[2], S Malzer[2], Y Simsek[2], P Müller[2], T Yamamoto[3] and K Kadowaki[3]

[1] Department of Physics, Izmir Institute of Technology, 35430 Urla Izmir, Turkey
[2] Department of Physics, Universität Erlangen-Nürnberg, D-91058, Erlangen, Germany
[3] Institute of Materials Science, University of Tsukuba, Tsukuba, Japan

E-mail: ozyuzer@iyte.edu.tr

Received 10 July 2012, in final form 26 September 2012
Published 17 October 2012
Online at stacks.iop.org/SUST/25/125004

Abstract
We fabricated rectangular mesa structures of superconducting $Bi_2Sr_2CaCu_2O_{8+d}$ (Bi2212) using e-beam lithography and Ar ion beam etching techniques for terahertz (THz) emission. *c*-axis resistance versus temperature (*R*–*T*), current–voltage (*I*–*V*) characteristics and bolometric THz power measurements were performed to characterize Bi2212 mesas. The emission frequency of mesas was determined using a Michelson interferometer setup which also demonstrates polarized emission. Interference patterns of THz radiation from Bi2212 mesas were detected by various detectors such as a liquid helium cooled silicon composite bolometer, a Golay cell and a pyroelectric detector. An emitted power as high as 0.06 mW was detected from Bi2212 mesas. For the first time, most of the pumped power was extracted as THz emission from a Bi2212 mesa. The radiation at 0.54 THz was detected using the Michelson interferometric setup.

(Some figures may appear in colour only in the online journal)

1. Introduction

Terahertz (THz) waves refer to electromagnetic radiation in the frequency interval from 0.1 to 10 THz. They interact with living matter without causing harmful photoionization, so it has potential for spotting the onset of tooth decay and skin or breast cancer using imaging. Their ability to penetrate materials that are usually opaque to both visible and infrared radiation also makes these waves so fascinating to scientists. The transmitted and reflected THz spectra of an enormous range of molecules contain THz absorption fingerprints and provide spectroscopic information. Spectroscopy in terahertz radiation makes the technique particularly useful for precise identification of drugs, detection of hidden explosives, and chemical and biological threats for defense and security applications [1]. Also, potential uses exist in ultra-high bandwidth wireless communication networks, vehicle control, atmospheric pollution monitoring and inter-satellite communication.

Although electromagnetic waves in the terahertz frequency region have a host of potential applications, these applications are presently limited by the lack of powerful, continuous wave, and compact solid-state sources [1]. There are some available CW sources such as quantum cascade lasers that only work above 1.2 THz [2]. Backward wave oscillators are bulky and have low output power at higher frequencies. Photomixing is also possible, but output power is again low. Schottky diodes are fairly compact but lacking in frequency agility and their cost is very high. The most powerful sources available are free-electron lasers. They produce either CW or pulsed beams of coherent THz waves [3]. However, they are not suitable for nonlaboratory applications due to their bulky size and high cost.

The Josephson effect, occurring between two superconductors separated by a thin insulating layer, provides a unique and simple principle to generate electromagnetic radiation in the terahertz frequency range. When a dc voltage is applied across the junction, an ac current oscillates at the Josephson frequency $f_{Jos} = V/\Phi_0$, where V is the voltage across the junction and Φ_0 is flux quantum. For instance, 1 mV corresponds to an emission frequency of 0.483 THz. Therefore, Josephson junctions are potential sources of

high-frequency electromagnetic radiation. Unfortunately, the operation frequency of a Josephson oscillator fabricated out of conventional superconductors is limited by the small superconducting energy gap [4]. Furthermore, the typical observed emission power is in the range of picowatts for a single junction. The emitted power can be enhanced using a large mutually coherent array of Josephson junctions made of conventional superconductors with various synchronization methods; however, variations of junction parameters may cause desynchronization and a significant drop in emission power [5].

Stacks of intrinsic Josephson junctions (IJJ) in layered high temperature superconductors, such as $Bi_2Sr_2CaCu_2O_{8+\delta}$ (Bi2212), offer the most promising alternative for terahertz oscillators. Since the junctions are homogeneous on the atomic scale along the *c*-axis of Bi2212 single crystals, a very high density of IJJs (one junction per 1.5 nm) makes the super-radiation possible with many junctions. Moreover, a large superconducting gap of 40 meV allows high Josephson frequencies up to 15 THz [6]. However, the major issue to synchronize oscillations in all junctions also remains for Bi2212 systems. To excite coherent electromagnetic radiation from intrinsic Josephson junctions, many approaches have been considered, among them the method of using moving Josephson vortices oscillating charge has been investigated most intensively [7]. Nevertheless, high-frequency emission was observed up to 0.5 THz from Bi2212 but with a weak power due to unsynchronized Josephson oscillations [8].

Recently, we observed continuous, coherent and monochromatic electromagnetic terahertz radiation emitted along the walls of rectangular mesa-shaped samples of the high-temperature superconductor Bi2212. The mesa acts as electromagnetic cavity, synchronizing almost all of the IJJ [9]. We observed that the fundamental frequencies of the emission were as high as 0.85 THz for a mesa width of 40 μm, providing an emitted power of up to 0.5 μW. More recently, emitted powers of 5 μW and frequencies at the higher harmonics up to 2.5 THz have been obtained [10]. The thermal management of the large mesas on Bi2212 crystals has been investigated by Kurter *et al* [11]. Furthermore, they showed that the back bending in the *I–V* curve results from the particular temperature dependence of quasiparticle resistances for Bi2212 rather than a significant suppression of the energy gap. The angular dependence of the emission power has also been studied [12]. Wang *et al* [13] imaged electric field distributions in the junction stack of Bi2212 by low-temperature scanning laser microscopy and observed standing electromagnetic waves (cavity resonances). They found that standing waves of the electric field are created through interactions with a hot spot and this effect may have an active role in generating synchronized radiation from intrinsic Josephson junction stacks. In [14] we discussed the dependence of the characteristics of the mesa structures on the oxygen doping level of the Bi2212 crystals and reported that the THz emitting mesas are below a certain underdoped level, which has a relatively small critical current in contrast to optimally doped and overdoped Bi2212. Minami *et al* [15] reported the radiation characteristics of terahertz radiation emitted from rectangular mesa structures of Bi2212 and they concluded that these devices exhibit enough frequency purity, intensity, and controllability to be suitable for device applications. Yuan *et al* [16] fabricate different shape mesa structure to overcome the synchronization problems, such as a trapezoidal cross-section which leads to a gradient in the critical currents of the IJJs. By improving the sample fabrication technique, Yamaki *et al* [17] estimated the total emission power of Bi2212 mesa structures to be about 30 μW.

Many theoretical models have been proposed to explain the nature of the mechanism of THz emission from Bi2212 mesas. Koshelev and Bulaevskii [18] proposed that modulations of the Josephson critical current along the width of mesa are responsible for the cavity resonance. A new dynamic state caused by the nonlinear property of IJJ has been discovered in which the phase kinks enable cavity resonance modes of the Josephson plasma [19, 20]. Tachiki *et al* [21] suggest that the energy of the nonradiative component of the magnetic field allows the determination of the orientation of the cavity resonance mode. However, there is no consensus about the precise nature of the synchronization mechanism.

THz detection from rectangular Bi2212 mesa structures nowadays is mostly accomplished with a liquid helium cooled Si composite bolometer, which has almost 10^{-14} W $Hz^{-1/2}$ NEP, due to the low emission power resulting from unsynchronized emission of Josephson junctions. Liquid helium cooled bolometers are sensitive detectors with a fast response, but their usage is difficult in nonlaboratory applications because they use liquid helium. THz detectors such as Golay cells and pyroelectric detectors don't need a cryogenic environment, so they have found common use in low-cost applications. However, their sensitivities are much lower than Si composite bolometers. They suffer from a slow response time and the maximum input power is limited to a few tens of μW [22]. The NEP values are in the range from 1 nW $Hz^{-1/2}$ to 10 nW $Hz^{-1/2}$ for Golay cells and pyroelectric detectors [23]. In this work, we show that Golay cells and pyroelectric detector can be used to detect THz from Bi2212 if sufficient power is obtained from synchronously emitting Josephson junctions.

2. Experimental details

In this study, single crystals of Bi2212 grown by the traveling solvent floating zone (TSFZ) technique were used. The as-grown crystals were cut in small pieces and annealed in partial O_2 pressure with slow and long processes for two days to obtain homogenous underdoped Bi2212 single crystals. After annealing, a piece of a small single crystal was glued on a sapphire substrate with silver epoxy. The crystals were cleaved using Scotch tape and then a 100 nm gold film was evaporated onto the crystal. Rectangular mesa structures (55×300 μm^2) with a height of 1250 nm, which corresponds to 833 junctions in a mesa, were fabricated on Bi2212 single crystals using e-beam lithography and Ar ion beam etching techniques. After the mesa fabrication, a CaF_2 layer was evaporated through a shadow mask onto the top part of the crystal, including a small section of the mesa for electrical

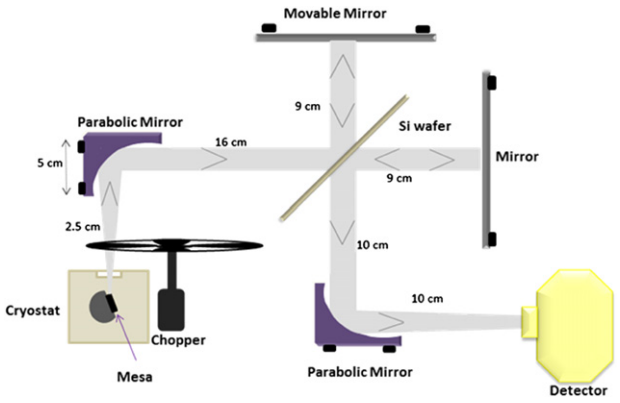

Figure 1. Michelson interferometer setup.

isolation purposes, in order to establish electrical contact to the gold layer on top of the mesa. A lift-off technique was used for fabrication of gold strips by e-beam lithography onto the mesa and the CaF_2. Finally, a gold wire was attached to the gold strip over the CaF_2 and two pads with silver epoxy for the electrical contacts of the mesa and two pads.

In order to characterize the Bi2212 mesas, *c*-axis resistance versus temperature (*R*–*T*) and *I*–*V* behavior were measured in a He flow cryostat. During *I*–*V* characterization, the emission characteristics of the mesas below T_c were also measured with a bolometer, Golay cell or a pyroelectric detector. A Michelson interferometer setup as shown in figure 1 was used to determine the emission frequency. First, a complete *I*–*V* curve is measured with one blocked mirror of the Michelson interferometer. The optimum emission voltage is obtained from these data. Then, the mesa is biased at this voltage and interferometric data are taken.

3. Results and discussion

Figure 2(a) shows the *I*–*V* curve of one of the representative THz emitting mesas with 55×300 μm^2 at $T = 35$ K. The trace was taken by both a back and forward scan. A large contact resistance between gold and Bi2212 is determined from the *I*–*V* curve. The data also shows that the Josephson current density is 103 A cm^{-2}, which is in the underdoped region of the Bi2212 phase diagram and comparable to other THz emitting mesas [13]. Figure 2(b), shows the detected THz radiation signals from a Si composite bolometer. At the back-bending region of *I*–*V* curve, only a small increment is observable in the bolometer response due to great emission peak power. This increment indicates that local temperature of the mesa is increasing and the bolometer detects the heating of the mesa in the form of unpolarized, incoherent blackbody radiation. When all junctions are in the resistive state and the bias is decreasing slowly, polarized and synchronized emission peaks from the mesa for positive and negative bias voltages were observed in the return branches at ± 1.28 V. On the bias decreasing part of the *I*–*V* curve at low bias there are some jumps (figure 2(a)). They occur as some junctions switch to the zero voltage state and they are referred to as re-trapping. When we look at the emission region (arrows in figure 2(a)), we see a bump in the return branch due to radiation (inset of figure 2(a)). That is, emission persists over an extended voltage range around the resonance condition. This property is a consequence of the slightly inclined side walls of the mesa resonator and allows the design of THz sources with voltage-tunable emission frequencies [24]. As can be seen from the close-up of the return branch, no re-trapping events were observed in the emission region, indicating that all junctions are tightly locked to the resistive state. The absence of a jump in the *I*–*V* curve allows us to establish a baseline of the current and to determine the excess current that supplies the energy for the excitation of the cavity resonance. These data suggest that about 126 μW is pumped into the in-phase resonance.

The frequency of the emission was determined by a simple interferometer setup, as shown in figure 1, implementing various detectors (bolometer, Golay cell and pyroelectric detector). The setup splits a single wave emitted from the long edge of the mesa so that one wave strikes a fixed mirror and the other a movable mirror. When the reflected beams are brought together, they form an interference pattern proving the coherence. Since the accuracy of the interferometer depends on the efficiency of the beam splitter, we used a Si wafer as a beam splitter because it has large refractive index and thus operates effectively in the terahertz region from 0.2 to 10 THz [25].

Figure 3 shows signals detected by the detectors in the interferometer setup. It can be clearly seen that signals detected by the Si composite bolometer have lower noise due to its higher sensitivity. Our bolometer has an NEP value of 10^{-13} W $Hz^{-1/2}$, but needs to work at liquid helium temperature. The cryogenic environment is not necessary for the Golay cell and the pyroelectric detector, however, their sensitivities are much lower than than Si composite bolometer. The NEP values are in the range of 1 nW $Hz^{-1/2}$ for the Golay cell and 60 nW $Hz^{-1/2}$ for the pyroelectric detector. Therefore, more noisy signals were observed from the pyroelectric detector. However, the fact that radiation could even be detected with the pyroelectric detector is proof of intense radiation.

The emission frequency was calculated by a fast Fourier transform (FFT) of the interference data given in figure 3 using the Labview program. Figure 4 shows the Fourier transform of the data, providing the frequency spectrum of the emission. The peak in this figure indicates that the emission frequency is 0.54 THz for all three different detector setups. The noise in the interferometer patterns of the pyroelectric detector also shows noise in the FFT spectrum. If we subtract the contact resistance from the *I*–*V* curve, the voltage of the bump decreases to 955 mV. According to the Josephson voltage–frequency relation, the emission frequency is 0.54 THz, which occurs at 955 mV for 833 junctions found from height of mesa. This is consistent with interferometer result, so it satisfies the Josephson voltage–frequency relation.

In order to estimate the emission power, first we calculated the signal to noise ratios from figure 4 and then

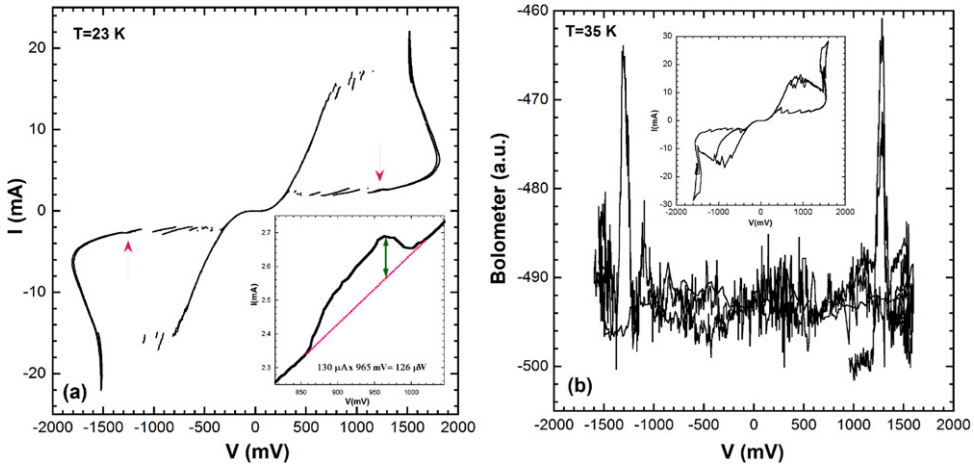

Figure 2. (a) Current versus voltage (I–V) curve of the mesa at 28 K. The inset shows the formation of a bump in I–V at the emission voltage. Note that the contact resistance is subtracted from I–V curve in order to estimate the exact pump energy. (b) Liquid helium cooled Si composite bolometer output versus voltage curve of the mesa at 35 K. The inset shows I–V curve of the mesa.

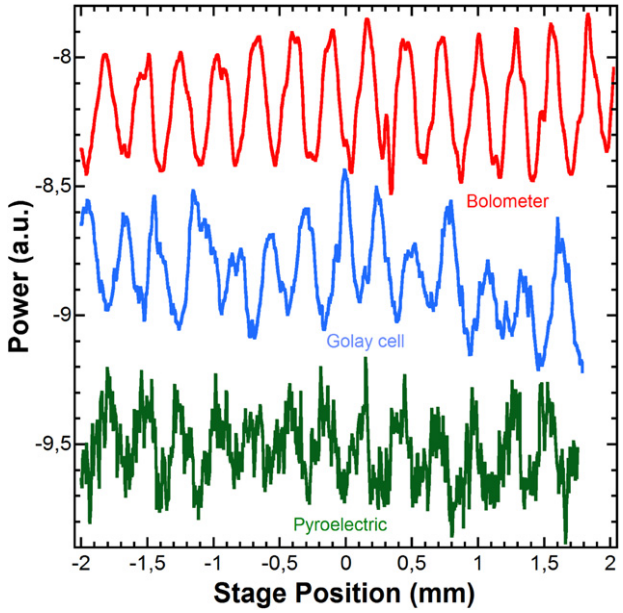

Figure 3. Interference patterns detected by bolometer, Golay cell, and pyroelectric detector.

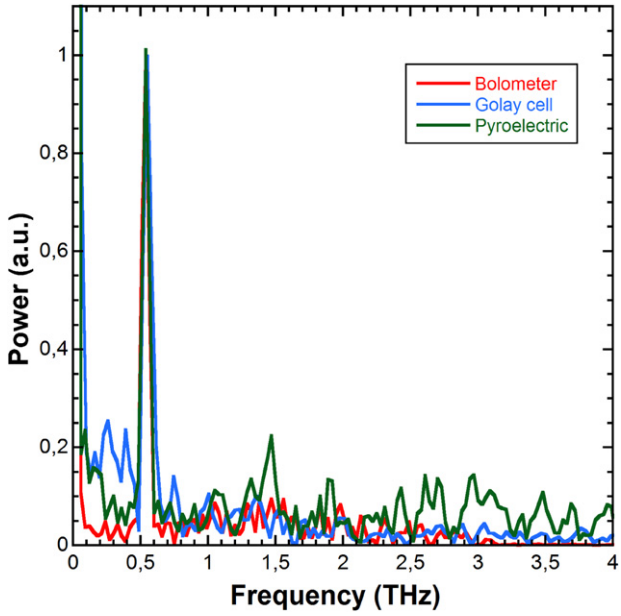

Figure 4. Fast Fourier transforms of interference patterns given in figure 3.

we determined the irradiance incident on the detectors using

$$H = \frac{\mathrm{NEP}}{A}\left(\frac{V_\mathrm{s}}{V_\mathrm{n}}\right)(\Delta f)^{1/2}, \qquad (1)$$

where H is the irradiance incident on the detector of area A, V_n is the root mean square noise voltage within the measurement bandwidth Δf, and V_s is the root mean square signal voltage [26]. We get nearly 270 nW emission power for the Golay cell and pyroelectric detector for 1 Hz bandwidth. We did not consider the bolometer response because fine structures make the determination of signal to noise ratio difficult. We calculated the total attenuation of THz waves in the 5 mm Si wafer and 2 mm polyethylene window as between 2.0% and 3.0% [27, 28]. When we take into account the geometrical configurations of the mesa, equipment and attenuation of THz waves in the Si wafer and polyethylene window, 270 nW emission power leads to a value between 23–60 μW total power. Since the attenuation of a THz waves in ambient air is nearly 1000 dB km^{-1} for 540 GHz, we did not consider attenuation in ambient air [29]. Since the pumped power is 126 μW, a maximum 47.6% of the total dc power is dissipated in the mesa. To the knowledge of the authors, this is the first time that most of the pumped power has been extracted as THz emission. In order to achieve synchronized oscillations in all junctions, the junction arrays must be highly uniform. Different junction parameters, especially the Josephson critical current, lead to desynchronization and a dramatic drop in emission power. The doping in Bi2212 substantially changes superconducting parameters such as the energy gap, critical current density, etc [6, 30]. We think that

the high quality of the crystal and increased annealing time to obtain more homogenous doping of underdoped Bi2212 is responsible for this high efficiency because the homogeneity of doping leads to a narrow band energy gap distribution and uniform structural and electrical characteristics.

4. Conclusion

THz detection from rectangular Bi2212 mesa structures nowadays is mostly accomplished with bolometers. In this paper, we showed that synchronously emitting Josephson junctions made from Bi2212 provide sufficient power to allow room temperature THz detectors, such as Golay cells and pyroelectric detectors, due to the high emitted power. We calculate that most of the pumped power is extracted as THz emission. The interference patterns were detected after traveling a long way through ambient air. The emission frequency calculated by a Fourier transformation of the interference data is consistent with the Josephson frequency–voltage relation. These THz emitting mesas can easily be used for practical applications as sub-THz sources without the need for high magnetic fields, such as in case of moving vortices or sub-THz operation of quantum cascade lasers (QCL) [31].

Acknowledgments

This research was supported in part by the TUBITAK (Scientific and Technical Council of Turkey) project number 110T248. L Ozyuzer acknowledges support from the Alexander von Humboldt foundation.

References

[1] Tonouchi M 2007 *Nature Photon.* **1** 97
[2] Wade A, Fedorov G, Smirnov D, Kumar S, Williams B S, Hu Q and Reno J L 2009 *Nature Photon.* **3** 41
[3] Saldin E L, Schneidmiller E A and Yurkov M V 2000 *The Physics of Free Electron Lasers* (*Advanced Texts in Physics*) (New York: Springer)
[4] Langenberg D N, Scalapino D J, Taylor B N and Eck R E 1965 *Phys. Rev. Lett.* **15** 294
[5] Barbara P, Cawthorne A B, Shitov S V and Lobb C J 1999 *Phys. Rev. Lett.* **82** 1963
[6] Ozyuzer L, Zasadzinski J F and Miyakawa N 1999 *Int. J. Mod. Phys.* B **13** 3721
[7] Bae M H, Lee H J and Choi J H 2007 *Phys. Rev. Lett.* **98** 027002
[8] Batov I E, Jin X Y, Shitov S V, Koval Y, Müller P and Ustinov A V 2006 *Appl. Phys. Lett.* **88** 262504
[9] Ozyuzer L *et al* 2007 *Science* **318** 1291
[10] Kadowaki K *et al* 2008 *Physica* C **468** 634
[11] Kurter C *et al* 2009 *IEEE Trans. Appl. Supercond.* **19** 428
[12] Kadowaki K, Tsujimoto M, Yamaki K, Yamamoto T, Kashiwagi T, Minami H, Tachiki M and Klemm R A 2010 *J. Phys. Soc. Japan* **79** 023703
[13] Wang H B, Guenon S, Yuan J, Iishi A, Arisawa S, Hatano T, Yamashita T, Koelle D and Kleiner R 2009 *Phys. Rev. Lett.* **102** 017006
[14] Ozyuzer L *et al* 2009 *Supercond. Sci. Technol.* **22** 114009
[15] Minami H, Kakeya I, Yamaguchi H, Yamamoto T and Kadowaki K 2009 *Appl. Phys. Lett.* **95** 232511
[16] Yuan J *et al* 2012 *Supercond. Sci. Technol.* **25** 075015
[17] Yamaki K, Tsujimoto M, Yamamoto T, Furukawa A, Kashiwagi T, Minami H and Kadowaki K 2011 *Opt. Express* **19** 3193–201
[18] Koshelev A E and Bulaevskii L N 2008 *Phys. Rev.* B **77** 014530
[19] Lin S, Hu X and Tachiki M 2008 *Phys. Rev.* B **77** 014507
[20] Lin S and Hu X 2008 *Phys. Rev. Lett.* **100** 247006
[21] Tachiki M, Fukuya S and Koyama T 2009 *Phys. Rev. Lett.* **102** 127002
[22] Liu H, Zhong H, Karpowicz N, Chen Y and Zhang X 2007 *Proc. IEEE* **95** 1514
[23] Rogalski A and Sizov F 2011 *Opto-Electron. Rev.* **19** 346
[24] Gray K E *et al* 2009 *IEEE Trans. Appl. Supercond.* **19** 886
[25] Homes C C, Carr G L, Lobo R P S M, LaVeigne J D and Tanner D B 2007 *Appl. Opt.* **46** 7884
[26] Ready J 2011 *Module 1.6 Fundamentals of Photonics* ed C Roychoudhuri (Bellingham, WA: SPIE Optical Engineering) p 211
[27] Grischkowsky D, Keiding S, Exter M V and Fattinger C 1990 *J. Opt. Soc. Am.* B **7** 10
[28] Hou L, Shi W, Xu M and Chen Y 2009 *Proc. SPIE* **7277** 727703
[29] Yang Y, Shutler A and Grischkowsky D 2011 *Opt. Express* **19** 8830
[30] Ozyuzer L, Zasadzinski J F, Gray K E, Kendziora C and Miyakawa N 2002 *Europhys. Lett.* **58** 589–95
[31] Preu S, Döhler G H, Malzer S, Wang L J and Gossard A C 2011 *J. Appl. Phys.* **109** 061301